FOUR-COMPONENT SCATTERING POWER DECOMPOSITION USING ROTATED COHERENCY MATRIX

PI No. 016
Yoshio Yamaguchi

Department of Information Engineering, Niigata University, 950-2181 Japan
yamaguch@ie.niigata-u.ac.jp, T/F: 025-262-6752

1. INTRODUCTION

Since the successful launch of ALOS in 2006, we have seen significant advances in the utilization of fully polarimetric SAR (PolSAR) data. We are now in the phase of PolSAR applications for sensing and monitoring the Earth's environment. Specific application areas include natural and man-made disaster monitoring, forest monitoring, crop assessment, oceanography, etc. In this report, a method of utilization of fully polarimetric data by means of target decomposition is given.

Target decomposition still remains a main topic of PolSAR research area. Comprehensive reviews have been presented by Lee [1] and Cloude and Pottier [2]. There are two kinds in the incoherent decomposition. One is the most widely used H/$\bar{\alpha}$/A method developed by Cloude and Pottier based on the eigenvalue analysis [3-6]. Touzi recently proposed a new incoherent decomposition by applying the coherent Kennaugh decomposition in Pauli basis [7-8]. The other is a physical scattering model-based method, first developed by Freeman and Durden [9]. Several methods have been proposed to this model-based decomposition [10-14]. These methods rely on the ensemble averaging of the coherency or covariance matrix.

In the incoherent analysis for PolSAR data, there are 9 real-valued independent parameters as the second order statistics of polarimetric information [1-2]. The physical scattering model tries to account for these 9 parameters. The three-component decomposition accounts for 5 terms [9]. The four-component scheme accounts for 6 parameters by adding a fourth component, the helix scattering [10]. An [11] and Yamaguchi [12] reduced the number of independent parameter from 9 to 8, by rotation of the measured coherency matrix, leaving unaccounted number as 2. The remaining 2 correspond to the real and imaginary part of T_{13} element in the coherency matrix, and they are small minor terms. These 2 parameters are not accounted in any physical model-based decomposition up to now [1] for complete matching.

In this report, we present some results of the four-component scattering power decomposition with rotation of coherency matrix applied to ALOS-PALSAR polarimetric data sets. We have seen a great improvement in polarimetric image by this new decomposition method.

2. FOUR-COMPONENT SCATTERING POWER DECOMPOSITION

Since coherency matrix and covariance matrix are Hermitian matrices and convertible each other through unitary transformation, we use coherency matrix formulation in the decomposition. The coherency matrix formulation has advantages in the mathematical operations as well as in the interpretation of physical scattering phenomena. Let's denote the coherency matrix as,

$$[T] = \begin{bmatrix} T_{11} & T_{12} & T_{13} \\ T_{21} & T_{22} & T_{23} \\ T_{31} & T_{32} & T_{33} \end{bmatrix} = \begin{bmatrix} T_{11} & T_{12} & T_{13} \\ T_{12}^* & T_{22} & T_{23} \\ T_{13}^* & T_{23}^* & T_{33} \end{bmatrix} \tag{1}$$

It should be noted that T_{11} , T_{22} and T_{33} are real-valued terms and that T_{12}, T_{13}, and T_{23} are complex valued. Therefore there are 9 real-valued parameters in the matrix.

The four-component scattering power decomposition divides polarimetric data of imaging pixel area into surface scattering, double bounce scattering, volume scattering, and helix scattering power with 4 expansion sub-matrices.

$$\langle [T] \rangle = P_s \langle [T] \rangle_{surface} + P_d \langle [T] \rangle_{double} + P_v \langle [T] \rangle_{vol} + P_c \langle [T] \rangle_{helix} \tag{2}$$

Eq. (2) is an extension of the three-component decomposition [9] to deal with non-reflection symmetry scattering case [10]. Sub-matrices in (2) are chosen so that the *Trace* becomes unity.

The expansion matrix for the surface scattering is

$$\langle [T] \rangle_{surface} = \frac{1}{1+|\beta|^2} \begin{bmatrix} 1 & \beta^* & 0 \\ \beta & |\beta|^2 & 0 \\ 0 & 0 & 0 \end{bmatrix}, \quad |\beta| < 1 \tag{3}$$

For the double bounce scattering, the expansion matrix is given by

$$\langle [T] \rangle_{bouble} = \frac{1}{1+|\alpha|^2} \begin{bmatrix} |\alpha|^2 & \alpha & 0 \\ \alpha^* & 1 & 0 \\ 0 & 0 & 0 \end{bmatrix}, \quad |\alpha| < 1 \tag{4}$$

where α *and* β are unknowns to be determined.

For the volume scattering, we choose one of the following matrices according to the magnitude balance of $\langle |S_{HH}|^2 \rangle$ and $\langle |S_{VV}|^2 \rangle$.

$$\langle [T] \rangle_{vol} = \frac{1}{30} \begin{bmatrix} 15 & 5 & 0 \\ 5 & 7 & 0 \\ 0 & 0 & 8 \end{bmatrix}, \quad \text{for } 10 \log \left(\langle |S_{VV}|^2 \rangle / \langle |S_{HH}|^2 \rangle \right) < -2\ dB \tag{5}$$

$$\langle [T] \rangle_{vol} = \frac{1}{4} \begin{bmatrix} 2 & 0 & 0 \\ 0 & 1 & 0 \\ 0 & 0 & 1 \end{bmatrix}, \quad \text{for } \left| 10 \log \left(\langle |S_{VV}|^2 \rangle / \langle |S_{HH}|^2 \rangle \right) \right| < 2\ dB \tag{6}$$

$$\langle [T] \rangle_{vol} = \frac{1}{30} \begin{bmatrix} 15 & -5 & 0 \\ -5 & 7 & 0 \\ 0 & 0 & 8 \end{bmatrix}, \quad \text{for } 10 \log \left(\langle |S_{VV}|^2 \rangle / \langle |S_{HH}|^2 \rangle \right) > 2\ dB \tag{7}$$

The helix scattering expansion matrix, which takes into account of the non-reflection symmetry condition, is

$$\langle [T] \rangle_{helix} = \frac{1}{2} \begin{bmatrix} 0 & 0 & 0 \\ 0 & 1 & \pm j \\ 0 & \mp j & 1 \end{bmatrix} \tag{8}$$

The surface scattering power P_s, the double bounce scattering power P_d, the volume scattering power P_v, and the helix scattering power P_c can be obtained directly from (2).

The three-component accounts for 5 parameters (T_{11},T_{22},T_{33},T_{12}) out of 9 independent parameters in the coherency matrix. Since the helix expansion matrix (8) accounts for Im (T_{23}) term in (1), the four-component method accounts for 6 parameters (the above 5 plus Im (T_{23}) term).

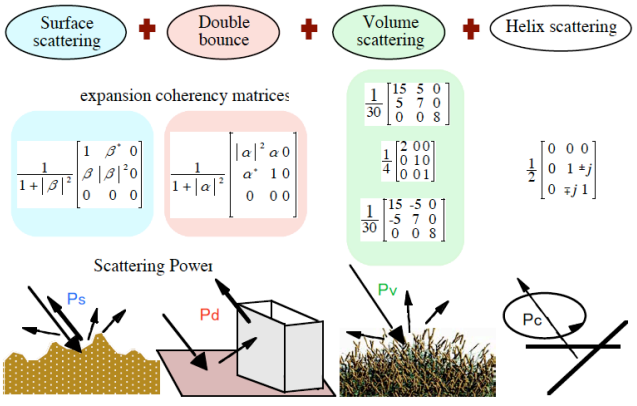

Fig. 1 Four-component scattering power decomposition using Coherency matrix

3. ROTATION OF COHERENCY MATRIX

The four-component decomposition has been successfully applied to imaging of POLSAR data using RGB color-coding. It provides us with intuitive imaging results by full color-coding, and with simple and easy calculation.

However, in the imaging process, we sometimes encounter problems of 1) negative power occurrence, and 2) difficulty in discriminating oriented urban area versus vegetation signatures because they have similar polarimetric responses. Man-made structures orthogonal to radar direction of illumination are decomposed into double bounce objects exhibiting "red" in the decomposed image. However, the oriented urban building blocks and houses with respect to radar illumination are decomposed into volume scattering objects exhibiting "green". Since "*green*" color is allotted for volume scattering, one may confuse the area as vegetation caused by volume scattering. Although they have strong backscattering power compared to those of vegetation, they are classified as "green" in case the RGB color-coding is used. It is desirable to classify obliquely oriented urban blocks/buildings as man-made structure (*red*) from the classification point of view.

The main reason for these problems 1) and 2) is too big *HV* component. In order to resolve these, we try to minimize the cross-polarized term T_{33} by a rotation of coherency matrix as shown in Fig. 2, which is directly related to avoid negative power problem.

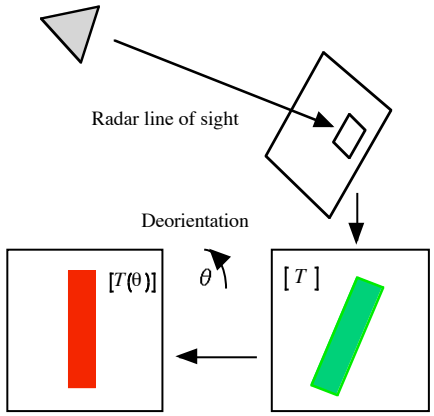

Fig. 2 Rotation concept

3.1 Rotation of Coherency Matrix

Rotation of the coherency matrix along the line of sight by angle θ is given by

$$[T(\theta)] = [R_P(\theta)]\,[T]\,[R_P(\theta)]^{\dagger} \tag{9}$$

$$[R_p(\theta)] = \begin{bmatrix} 1 & 0 & 0 \\ 0 & \cos 2\theta & \sin 2\theta \\ 0 & -\sin 2\theta & \cos 2\theta \end{bmatrix} \tag{10}$$

We denote the rotated coherency matrix as

$$[T(\theta)] = \begin{bmatrix} T_{11}(\theta) & T_{12}(\theta) & T_{13}(\theta) \\ T_{21}(\theta) & T_{22}(\theta) & T_{23}(\theta) \\ T_{31}(\theta) & T_{32}(\theta) & T_{33}(\theta) \end{bmatrix} \quad (11)$$

3.2 Minimization of T33

The T_{33} term in (11) can be written as

$$T_{33}(\theta) = T_{33} \cos^2 2\theta - \mathrm{Re}\,(T_{23}) \sin 4\theta + T_{22} \sin^2 2\theta \quad (12)$$

Forcing the derivative with respect to θ to be zero ($T_{33}^{'}(\theta) = 0$) yields the rotation angle as

$$\tan 4\theta = \frac{2\,\mathrm{Re}\,(T_{23})}{T_{22} - T_{33}} \quad (13)$$

$$2\theta = \frac{1}{2} \tan^{-1}\left(\frac{2\,\mathrm{Re}\,(T_{23})}{T_{22} - T_{33}}\right) \quad (14)$$

The expression (14) is of the same form as the phase of the correlation coefficient in the circular polarization basis [4], which is also used for surface slope estimation [13] as well as orientation angle compensation [14].

After this rotation, the elements of the coherency matrix become;

$$T_{11}(\theta) = T_{11} \quad (15)$$

$$T_{12}(\theta) = T_{12} \cos 2\theta + T_{13} \sin 2\theta \quad (16)$$

$$T_{13}(\theta) = T_{13} \cos 2\theta - T_{12} \sin 2\theta \quad (17)$$

$$T_{23}(\theta) = j\,\mathrm{Im}\,(T_{23}) \quad (18)$$

$$T_{22}(\theta) = T_{33} \cos^2 2\theta + T_{22} \sin^2 2\theta + \mathrm{Re}(T_{23}) \sin 4\theta \quad (19)$$

$$T_{33}(\theta) = T_{33} \cos^2 2\theta + T_{22} \sin^2 2\theta - \mathrm{Re}(T_{23}) \sin 4\theta \quad (20)$$

It is seen that $T_{11}(\theta)$ remains the same, $T_{33}(\theta)$ decreases by $\mathrm{Re}(T_{23}) \sin 4\theta$, and that $T_{22}(\theta)$ increases the same amount by this rotation. It should be noted that $T_{23}(\theta)$ becomes pure imaginary, which exactly fits the helix scattering model. This rotation causes $\mathrm{Re}\,(T_{23}(\theta))$ to be zero, which means the number of independent parameter reduced from 9 to 8. Therefore, the combination of the rotation of coherency matrix and the four-component decomposition accounts 6 terms out of 8 independent parameters.

The remaining 2 terms correspond to the real and imaginary part of $T_{13}(\theta)$ element of (17). They become small minor terms compared to the original T_{13}.

4. DECOMPOSITION SCHEME

The decomposition with the rotated coherency matrix can be written in a similar way to (2);

$$\langle [T(\theta)] \rangle = P_s \langle [T] \rangle_{surface} + P_d \langle [T] \rangle_{double} + P_v \langle [T] \rangle_{vol} + P_c \langle [T] \rangle_{helix} \quad (21)$$

The schematic decomposition algorithm is provided in Fig. 3. The rotation of coherency matrix can be performed before the decomposition without loss of generality. Then we apply the four-component decomposition. It should be noted in the algorithm that all terms are directly derivable from the coherency matrix elements only.

Color-coded decomposed images of Kyoto are shown in Fig. 4 with before and after rotation of the coherency matrix for the sake of comparison. Several decomposed images are shown in Fig. 5, which are self-explanatory.

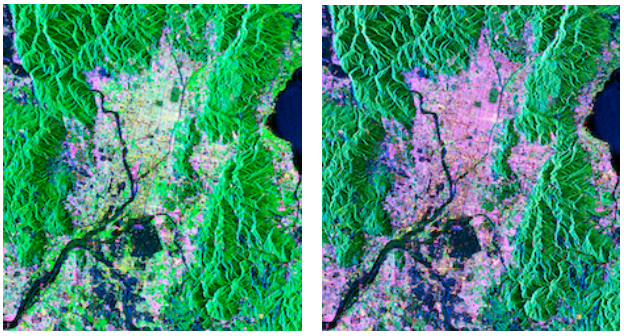

(a) Original (before rotation) (b) after T33 rotation

Fig. 4 Color-coded polarimetric images of Kyoto with R: double bounce, G: volume, B: surface scattering (Data no. ALPSRP172780690, level 1.1)

5. CONCLUSION

The four-component scattering power decomposition with rotation of coherency matrix is presented. By minimizing the cross-polarized component, the rotation angle is retrieved. This decomposition accounts for 6 parameters out of 8 independent polarization parameters. Although 2 parameters are left, they are usually very small and minor terms for complete decomposition. This decomposition scheme has several advantages;

1. The resultant decomposed image is quite in good agreement with actual situation seen by Google Earth image.
2. It is possible to discriminate oriented urban blacks or man-made structure from vegetation, which was previously difficult to be discriminated.
3. The image quality increased compared with the original decomposition within the fixed specification frame of radar resolution.
4. The decomposed image can be used for comparison of time series images because the image is always based on the minimization of the HV component as shown in Fig. 5.
5. The decomposition algorithm is simple and effective, since the calculation is carried out by the coherency matrix term only (Fig. 3).

By using this new decomposition method, it will be possible to create full-color polarimetric images which are comprehensive to everybody. Since each color represents physical scattering mechanism, it is easy to understand and classify objects in polarimetric images.

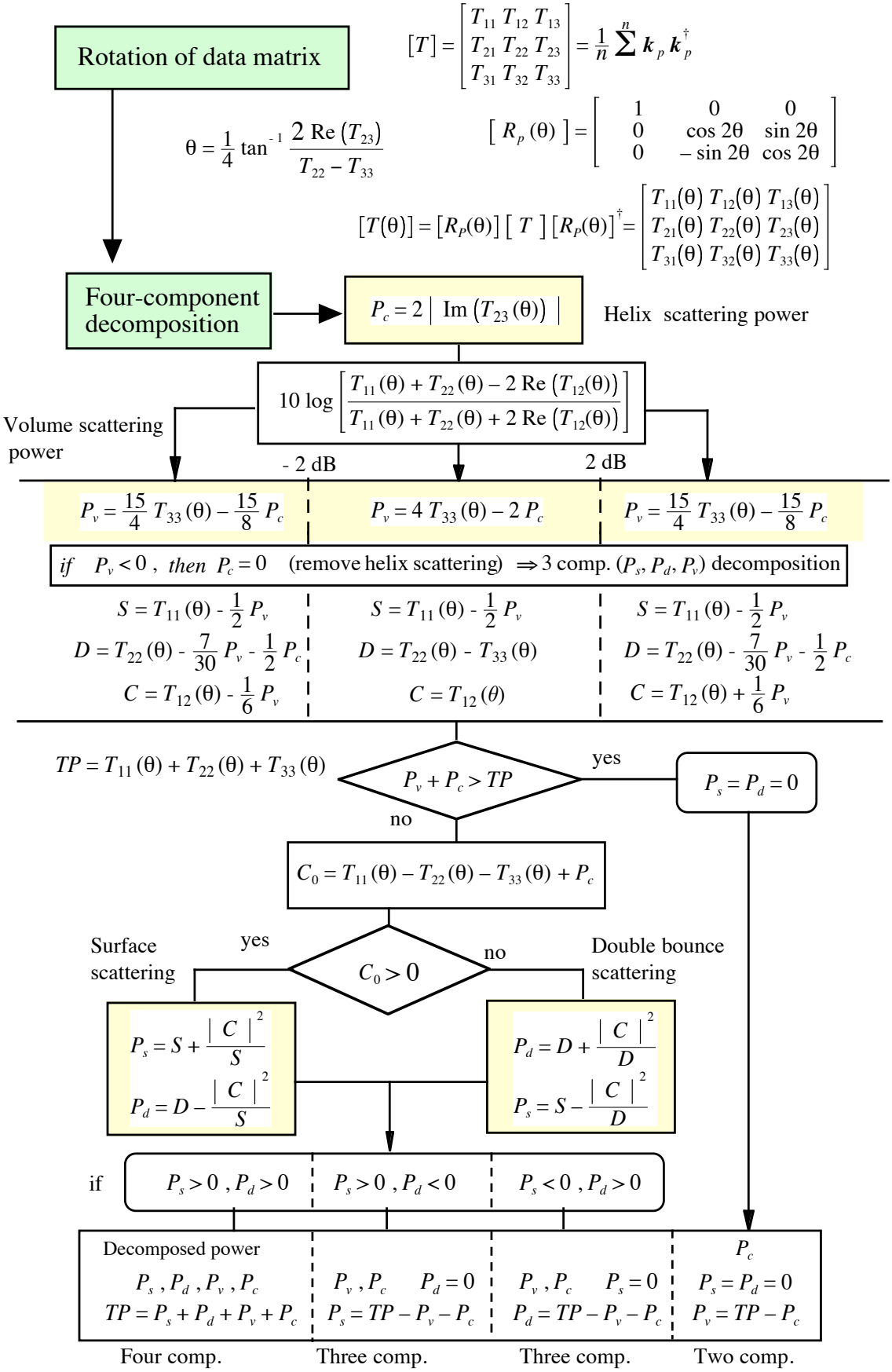

Fig. 3 Decomposition algorithm

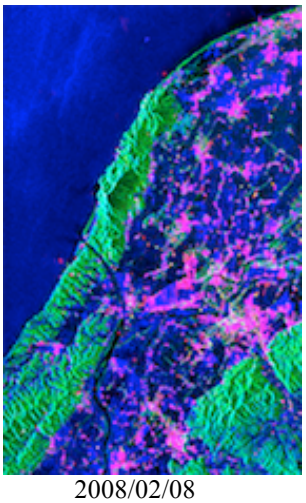

2008/02/08
ALPSRP108450750

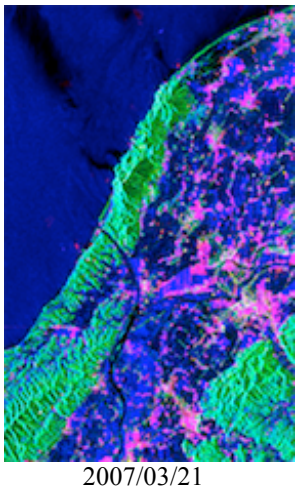

2007/03/21
ALPSRP061480750

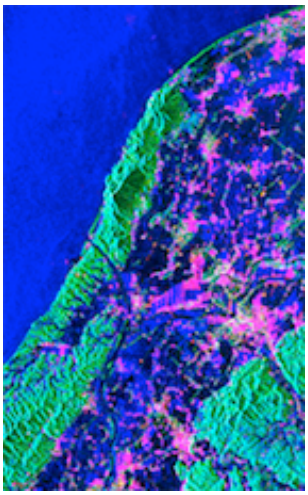

2010/03/29
ALPSRP222520750

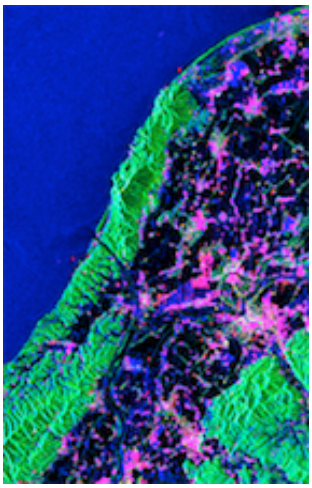

2007/05/06
ALPSRP068190750

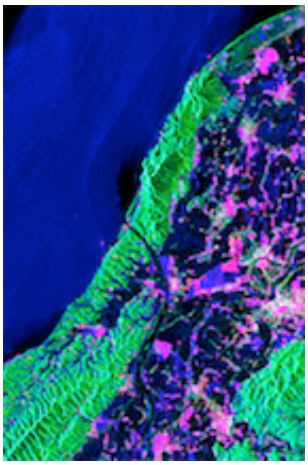

2006/06/18
ALPSRP021220750

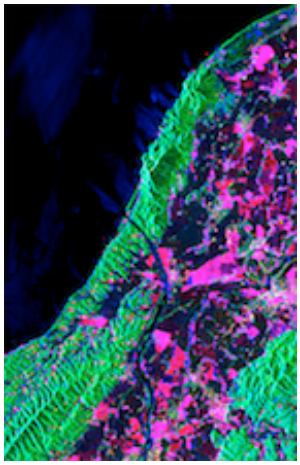

2006/08/03
ALPSRP027930750

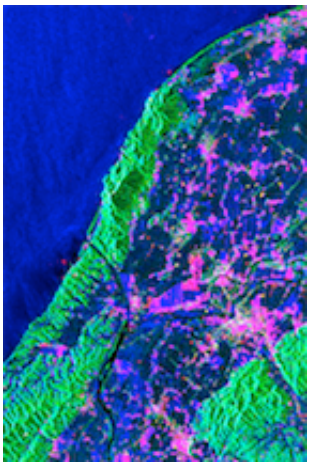

2007/11/06
ALPSRP095030750

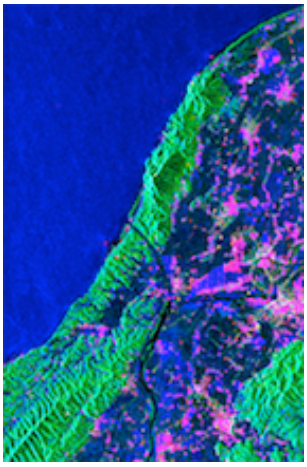

2008/11/08
ALPSRP148710750

Google Earth image of Semeru, Indonesia

Google Earth image of Tomakomai, Hokkaido, Japan

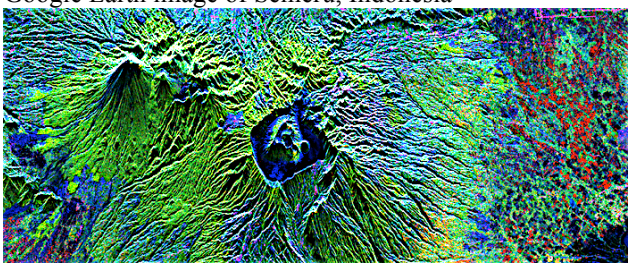

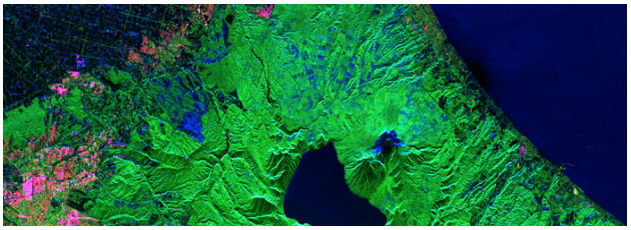

Fig. 5 Color-coded decomposed images by the four-component scattering power decomposition with 2 x 12 window and T_{33} rotation. Red: double bounce scattering, Blue: surface scattering, Green: volume scattering

Acknowledgment

The authors are grateful to JAXA for providing L-band ALOS-PALSAR PLR data sets continuously during JAXA/EORC/ALOS project.

6. REFERENCES

[1] J. S. Lee and T. Aisworth, "An overview of recent advances in polarimetric SAR information extraction: algorithms and applications," *Proc. of IGARSS 2010*, pp. 851-854, 2010

[2] S. R. Cloude and E. Pottier, "A review of target decomposition theorems in radar polarimetry," *IEEE TGRS,* vol. 34, no. 2, pp. 498-518, March 1996.

[3] E. Pottier, and J. S. Lee, "Application of the <<H/A/alpha>> polarimetric decomposition theorem for unsupervised classification of fully polarimetric SAR data on the Whishart distribution," *Proc. of EUSAR2000*.

[4] J. S. Lee and E. Pottier, *Polarimetric radar imaging from basics to applications,* CRC Press, 2009

[5] S. R. Cloude, *Polarisation: applications in remote sensing,* Oxford University Press, Oxford, New York, 2010

[6] D. Massonnet and J-C. Souyris, *Imaging with Synthetic Aperture Radar*, Taylor & Francis/CRC Press, New York, 2008.

[7] R. Touzi, "Target scattering decomposition in terms of roll-invariant target parameters," *IEEE TGRS*, vol. 45, Jan. 2007.

[8] R. Touzi, A. Deschamps, G. Rother, "Phase of target scattering for wetland characterization using polarimetric C-band SAR," *IEEE TGRS*, vol. 47, Sept. 2009.

[9] A. Freeman, and S. Durden, "A three-component scattering model for polarimetric SAR data," *IEEE TGRS,* vol. 36, no. 3, pp. 963-973, May 1998.

[10] Y. Yajima, Y. Yamaguchi, R. Sato, H. Yamada, and W. –M. Boerner, "POLSAR image analysis of wetlands using a modified four-component scattering power decomposition," *IEEE TGRS*, vol. 46, no. 6, pp. 1667-1673, Jun. 2008.

[11] W. An, Y. Cui, J. Yang, "Three-component model-based decomposition for polarimetric SAR data," *IEEE TGRS*, vol. 48, no. 6, pp. 2732-2739, 2010

[12] Y. Yamaguchi, A. Sato, R. Sato, H. Yamada, W. –M. Boerner, "Four-component scattering power decomposition with rotation of coherency matrix," *Proc. of IGARSS 2010*, pp.1327-1330, 2010

[13] J. S. Lee, D. L. Schuler, T. L. Ainsworth, E. Krogager, D. Kasilingam, W. -M. Boerner, "On the estimation of polarization orientation shifts induced by terrain slopes," *IEEE TGRS.,* vol. 40, no. 1, pp. 30-41, Jan. 2002.

[14] J. S. Lee and T. Ainsworth, "The effect of orientation angle compensation on coherency matrix and polarimetric target decompositions," *Proc. of EUSAR 2010*, Germany, 2010

[15] J. S. Lee, E. Krogager, T. L. Ainsworth, W. -M. Boerner, "Polarimetric analysis of radar signature of a manmade structure," *IEEE Geosci. Remote Sens. Letters,* vol.3, no. 4, pp. 555-559, Oct. 2006.

[16] Y. Yamaguchi, *Radar polarimetry from basics to applications* (in Japanese), IEICE, 2007

[17] Y. Yamaguchi, A. Sato, W. –M. Boerner, R. Sato, H. Yamada, "Four-component scattering power decomposition with rotation of coherency matrix," *IEEE TGRS,* vol. 47, no. 7, 2011 (in press).